APPLIED SCIENCES AND ENGINEERING

Fast-moving soft electronic fish

Tiefeng Li,[1,2*†] Guorui Li,[1*] Yiming Liang,[1] Tingyu Cheng,[2] Jing Dai,[2] Xuxu Yang,[1] Bangyuan Liu,[2] Zedong Zeng,[2] Zhilong Huang,[1,2†] Yingwu Luo,[2,3] Tao Xie,[3] Wei Yang[1]

Soft robots driven by stimuli-responsive materials have unique advantages over conventional rigid robots, especially in their high adaptability for field exploration and seamless interaction with humans. The grand challenge lies in achieving self-powered soft robots with high mobility, environmental tolerance, and long endurance. We are able to advance a soft electronic fish with a fully integrated onboard system for power and remote control. Without any motor, the fish is driven solely by a soft electroactive structure made of dielectric elastomer and ionically conductive hydrogel. The electronic fish can swim at a speed of 6.4 cm/s (0.69 body length per second), which is much faster than previously reported untethered soft robotic fish driven by soft responsive materials. The fish shows consistent performance in a wide temperature range and permits stealth sailing due to its nearly transparent nature. Furthermore, the fish is robust, as it uses the surrounding water as the electric ground and can operate for 3 hours with one single charge. The design principle can be potentially extended to a variety of flexible devices and soft robots.

INTRODUCTION

Conventional robots consisting of rigid components play essential roles in the modern time because of their high output force, precision, and controllability. However, these "hard" machines typically present limited adaptability. With the future hinging increasingly on their fusion with the complex operating environments, robots that are soft and deformable have become a necessity (*1*–*6*). Soft-bodied animals become important inspiration for designing soft robots that are geometrically adaptable and resilient to environments (*7*–*11*), safe to humans (*6*, *12*, *13*), and biopowered (*14*, *15*). In particular, mimicking the exceptional agility of insects (*16*, *17*), fish (*18*), octopuses (*19*, *20*), and snakes (*21*) has been a longtime pursuit. This task remains challenging given the difficulty in controlling high-performance soft actuators, especially when the device integration is taken into account.

Soft robots can be powered by either rigid electric motors (pumps) or stimuli-responsive soft actuators (*1*). We herein define them as soft motor-based robots and soft actuator-based robots (SARs). The former takes full advantages of the high energy density and efficiency of the motors. However, the intrinsic limitation of the motors prohibits their integration in a flexible, lightweight, and compact fashion, which is extremely desirable for soft robots. Typical stimuli-responsive actuators include ionic polymer metal composites (IPMCs) (*21*, *22*), dielectric elastomers (DEs) (*23*–*26*), shape memory alloys (SMAs) (*10*), responsive hydrogels (*27*, *28*), pneumatic structures (*13*), chemical reaction–inflated fluidic networks (*20*), and living cells (*14*, *15*). Although their power and precision are not comparable to motors, stimuli-responsive actuators offer unique advantages in high deformability and adaptability because of their excellent compliance. The central issue is to create a highly compact system combining actuation, power, and control while maintaining the softness of the entire robot (*1*, *4*, *20*). At present, simultaneous achievements of untethered powering and high speed are challenging for SARs. Among the natural inspirations for designing soft robots, aquatic creatures stand out because of their exceptional large fraction of soft body and high agility (*20*, *21*, *29*–*44*). The interest to create aquatic robots is further fueled by the mounting importance of ocean missions. However, aquatic robots present additional challenges in that high adaptability is required for operating in the complex ocean environments. Previous attempts to create aquatic SARs showed promise in their geometrically adaptability yet encountered difficulty in achieving high speed. The reported aquatic SARs can reach speeds up to 0.35 body length per second driven by SMAs (*32*) and 0.25 body length per second driven by IPMCs (*35*).

DEs stand out among various soft actuators for their exceptionally fast response and large actuation (*26*, *45*–*50*). However, the requirements for high voltages and rigid support frames prohibit their use in designing untethered SARs. In particular, achieving high-voltage insulation for a highly compact aqueous SAR appears to be an insurmountable obstacle. Here, we designed a manta ray–inspired DE-driven soft electronic fish. Contrary to the common belief that the entire DE assembly should be fully insulated, our design uses the surrounding open water as the electrode, taking full advantages of its weak yet sufficient electric conductivity. We find that water can function as the electric ground, thus resolving the need for further insulation. In addition, we use a highly compact electronic system for both remote control and the voltage boosting (3.7 V from a small battery to 10 kV). The overall design is compact and robust, achieving a swimming speed of 0.69 body length per second, about twice as fast as previously reported untethered aqueous SARs (*32*).

Inspired by the structure and propulsion mechanism of flapping pectoral fins, we design the electronic fish with DE membranes (3M VHB) as the muscle, silicone thin film as the fin, and a silicone frame as the elastomeric body. The detailed fabrication process is shown in Fig. 1. The muscle laminate consists of a thin hydrogel film as one electrode encapsulated between the two prestretched DE membranes, along with a small piece of tin foil as the electric feed line. The muscle and fin laminates (Fig. 1, A and B) are stacked together (Fig. 1C), with acrylonitrile butadiene styrene (ABS) frames as the mold. The curing of the silicone precursor in the mold forms the body (Fig. 1D) that bonds the muscle and fin together. Upon removing the ABS mold, the prestretched muscle shrinks. Constrained by the silicon body on one side, the muscle and body assembly bends into a buckled shape with a characteristic curvature (Fig. 1E). A silicone steering tail (Fig. 1F) with an embedded electromagnet is installed,

[1]Department of Engineering Mechanics, Zhejiang University, Hangzhou 310027, China. [2]Key Laboratory of Soft Machines and Smart Devices of Zhejiang Province, Zhejiang University, Hangzhou 310027, China. [3]State Key Laboratory of Chemical Engineering, College of Chemical and Biological Engineering, Zhejiang University, Hangzhou 310027, China.
*These authors contributed equally to this work.
†Corresponding author. Email: litiefeng@zju.edu.cn (T.L.); zlhuang@zju.edu.cn (Z.H.)

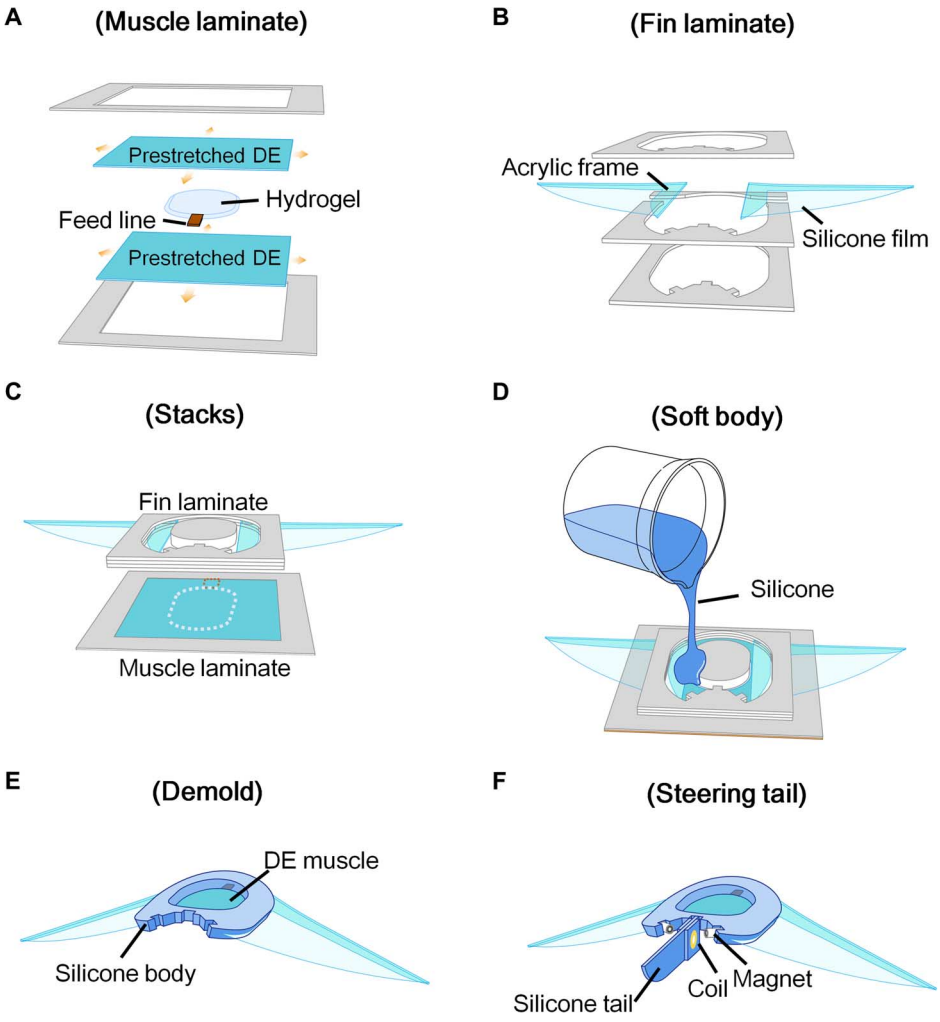

Fig. 1. Fabrication of electro-ionic fish. (**A**) Muscle laminate fabrication: A thin hydrogel film electrode was sandwiched between two biaxially prestretched (3 × 3) DE membranes (VHB membrane; initial thickness, 1.5 mm); the assembly was then fixed within ABS frames. (**B**) Fin fabrication: Two silicone films (thickness, 0.5 mm) and two rigid "L"-shaped acrylic frames (thickness, 1 mm) were glued together to form two pectoral fins, which were placed between two ABS frames. (**C**) The fin and muscle laminates were stacked together. The white and brown dashed lines indicate the locations of encapsulated hydrogel and feed line by DE membranes. (**D**) Liquid silicone precursor was poured into the mold (ABS frames) to fabricate the soft body. (**E**) The soft body bends after demolding. (**F**) Installation of the silicone tail and electromagnets.

which completes the fabrication of the fish. This design allows us to first connect the electronic fish with wired power to evaluate its performance, and then integrate the onboard system for power and remote control. More details of the fabrication and assembly can be found in figs. S1 to S5. All components of the electric fish are soft and transparent, except the tiny electromagnets and the leading edges of the fins. The fabrication process is amendable to use three-dimensional (3D) printing to produce certain components of the soft electronic fish. Preliminary attempts are described in fig. S6.

Figure 2 shows the actuation mechanism of the electronic fish. Whereas the encapsulated hydrogel serves as an ionically conductive electrode (*50*), an important aspect of the design is to use the surrounding tap water as the other electrode. Despite the low electrical conductivity of the tap water (~50 mS/m), it is sufficient to serve as an effective electrode, as will be evidenced later in the context. The use of open water as the electrode is counterintuitive because the high voltage required to actuate DEs often raises safety concerns even in a dry and isolated environment. Contrary to such a conception, water serves an additional role as an electric ground, which improves the system robustness. Without applying a voltage, the muscle and the body maintain an equilibrium bending state (rest state) (Fig. 2A). When a voltage is applied (Fig. 2B), positive and negative charges accumulate on both sides of the DE, inducing Maxwell stress (*48*) that deforms the DE membranes. The net effect is a reduction on the body curvature, corresponding to the actuated state. The structural deformations with and without voltage are simulated by a finite element analysis (FEA) (details in the Supplementary Materials). Figure 2 (C to F) illustrates the bending angles corresponding to the rest and the actuated states, respectively. When a cyclic voltage is applied, the fins flap and the electronic fish can operate like a manta ray that generates thrust through periodic flapping pectorals.

RESULTS

The goal of this study is to achieve an untethered electronic fish with onboard power and control. As a first step, we perform a series of experiments to evaluate its performance under wired power. Here,

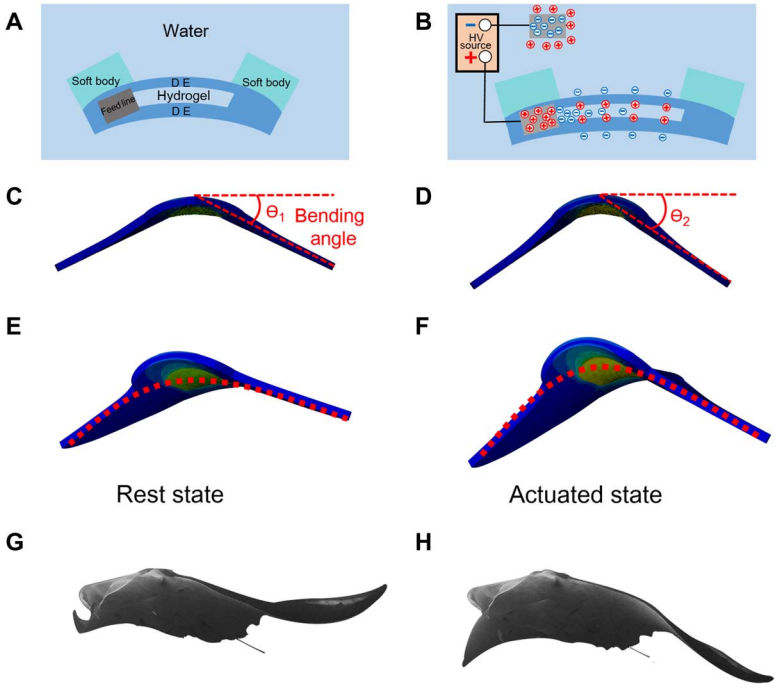

Fig. 2. Operation mechanism of electro-ionic fish. Front view of the actuating mechanisms. (A) In water, the soft body (silicone body) and the muscle laminates (two DE membranes and one hydrogel film) are deformed by the shrinking of the prestretched DE membranes with a bending curvature. (**B**) When a high voltage (HV) is applied to the muscle laminates, the electric field drives the ions in both the surrounding water and the hydrogel. Positive and negative charges accumulate on both sides of the DE membranes, inducing Maxwell stress and relaxing the DE membranes. The bending of the electro-ionic fish decreases. The surrounding water functions as the electric ground. (**C**) Front view (FEA) of the robotic fish in the rest state with a large bending angle θ_1. (**D**) Front view (FEA) for the actuated state of the robotic fish with a small bending angle θ_2. (**E**) Tilted view of FEA simulation for the rest state of the robotic fish. (**F**) Tilted view of FEA simulation for the actuated state of the robotic fish. Red dashed curves indicate the variation of bending. (**G**) Snapshot (similar tilted view) of a swimming manta ray. The body and fins of the manta ray buckle down with a large bending angle and (**H**) a small bending angle.

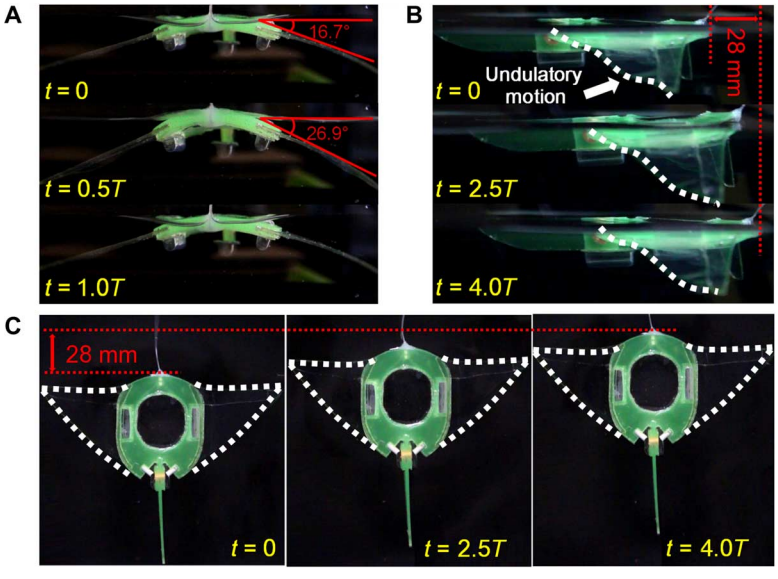

Fig. 3. Live snapshots of the swimming fish with wired power. $t = 0$ is defined as the beginning of the cycle with the fin in the actuated state, and T represents the time required for one full flapping cycle. (**A**) Bending variations of the soft body and fins (front views). (**B**) Forward motion of the fish and undulatory motion of the fins (side views; the white dashed lines highlight the fin edges). (**C**) The top views correspond to (B).

we focus on how the fish swims at the surface of the water by attaching buoys to the fish (details can be found in fig. S5). Accordingly, the wired fish (dyed in green for contrast) is recorded with live snapshots (Fig. 3), in the act of swimming under a square wave voltage (8 kV and 5 Hz), with the corresponding video in movie S1. Consistent with the simulation results, the fish body deforms between the actuated and the rest states, resulting in a change of bending angles from 16.7° to 26.9° (Fig. 3A), that is, flapping. This flapping motion is similar to that of a

manta ray (a detailed comparison can be found in section S3). We emphasize that this simple flapping is not sufficient for the forward motion. In our design, the rigid L-shaped leading edges of the fins are critical. The up-and-down flaps of rigid edges lead to undulatory motions of the soft silicone membrane (Fig. 3B and movie S2), resulting in the forward propulsion. Accordingly, the simple in-plane DE actuation is transformed into the necessary complex motions, similar to the working principle of motor transmission systems for cars, albeit in a compact and soft form. The tail, which remains in the middle position throughout the operation, ensures forward motion without turning (Fig. 3C).

With the wired power, an input AC voltage signal is amplified, which then actuates the fish and generates the thrust (Fig. 4A). The swimming speed is determined by the amplitude and frequency of the applied voltage. At any given amplitude, the corresponding speed-frequency curve shows multiple peaks (Fig. 4B). This nonmonotonic correlation is the result of the complex variation of the thrust and the hydrodynamic drag at different frequencies. Qualitatively, the thrust can be treated as the product of the frequency and the flapping amplitude (*51*). Even if the voltage amplitude is fixed, the flapping amplitude varies with the frequency due to the resonant behavior of the fish body and the nonlinear hydrodynamic drag. The swimming speed increases with the voltage amplitude, reaching the highest value of 13.5 cm/s at 10 kV and 5 Hz. With the fish body length of 9.3 cm, such a speed corresponds to 1.45 body length per second, much higher than previously reported values (<0.8 body length per second) for tethered swimming SARs (*51*). Besides swimming in a straight line, steering the tail through the electromagnets allows the fish to make turns. We measure the turning radii at various applied voltages and frequencies with the tail at full rudder, and the results are presented in table S1. Overall, the minimum turning radius achieved is 8.5 cm at 7 kV and 8 Hz, illustrating its high agility.

We develop a method to estimate the power and power efficiency of the electronic fish. When it swims at a constant speed v, the thrust force F_T equals the drag force F_D. The input electrical power P_{input} for DE actuation is partly converted into the mechanical power P_{output} to maintain the constant speed. Without considering the loss in the voltage amplifier and circuits, P_{input} can be estimated as the product between the electrical energy difference and the operating frequency f

$$P_{input} = (C_{act} - C_{rest})\Phi^2 f \quad (1)$$

C_{act} and C_{rest} are the capacitances of the DE in the actuated and rest states. Φ is the amplitude of the applied voltage. P_{output} can be calculated as

$$P_{output} = vF_D \quad (2)$$

The power efficiency η at a constant swimming speed can be expressed as

$$\eta = P_{output}/P_{input} \quad (3)$$

All variables and parameters in Eqs. 1 to 3 can be measured experimentally, thus allowing the calculations of power and power efficiency under different operating conditions (see fig. S7 and table S2). For the highest speed (13.5 cm/s) achieved at 10 kV and 5 Hz, the corresponding input power and power efficiency are 0.024 W and 10.25%, respectively. As a reference, a rainbow trout (body length of about 25 cm) has an input power of 0.03 W at a speed of 10 cm/s (*52*). Thus, both the power and the speed of our electronic fish are comparable to those of the real fish of similar size.

We next address a major challenge for SARs, that is, achieving onboard power and control while maintaining a considerable portion of its performance. We first engineer a lightweight and compact system

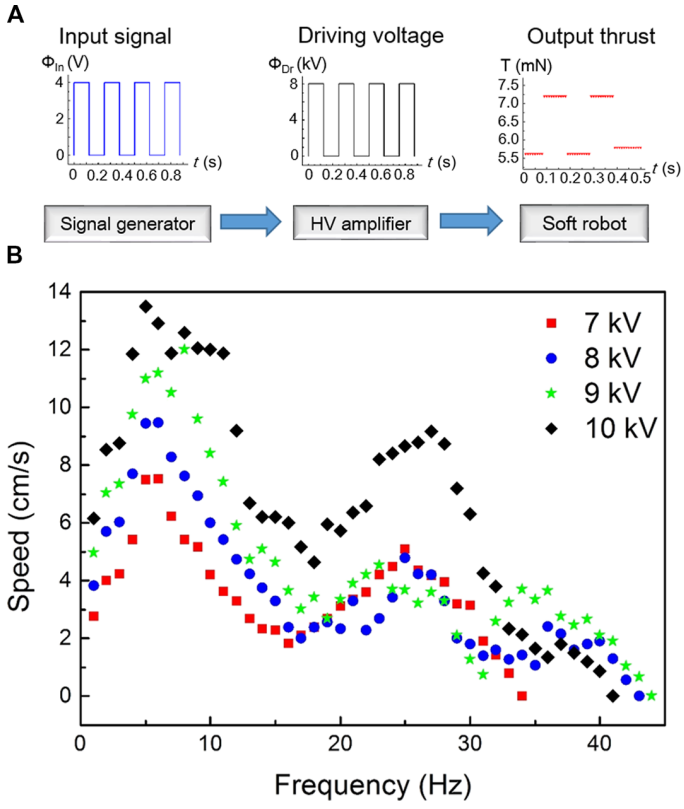

Fig. 4. Quantitative performance evaluation via wired power. (**A**) Voltage signal from the signal generator is amplified through a high-voltage amplifier and fed to the soft robotic fish. (**B**) The speed of robotic fish demonstrates a double peak distribution and reaches a maximum of 13.5 cm/s.

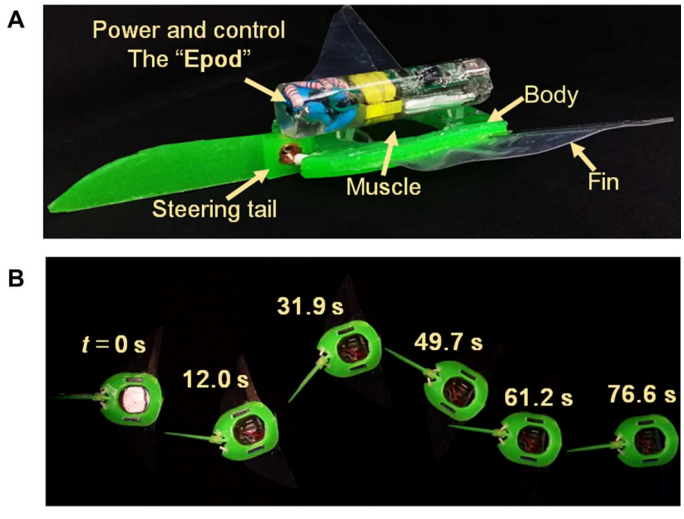

Fig. 5. Performance of the untethered fish. (**A**) Tilted view of the fish showing the onboard system for power and remote control. (**B**) Live snapshots of the swimming of the robotic fish under remote control (voltage of 8 kV and 5 Hz).

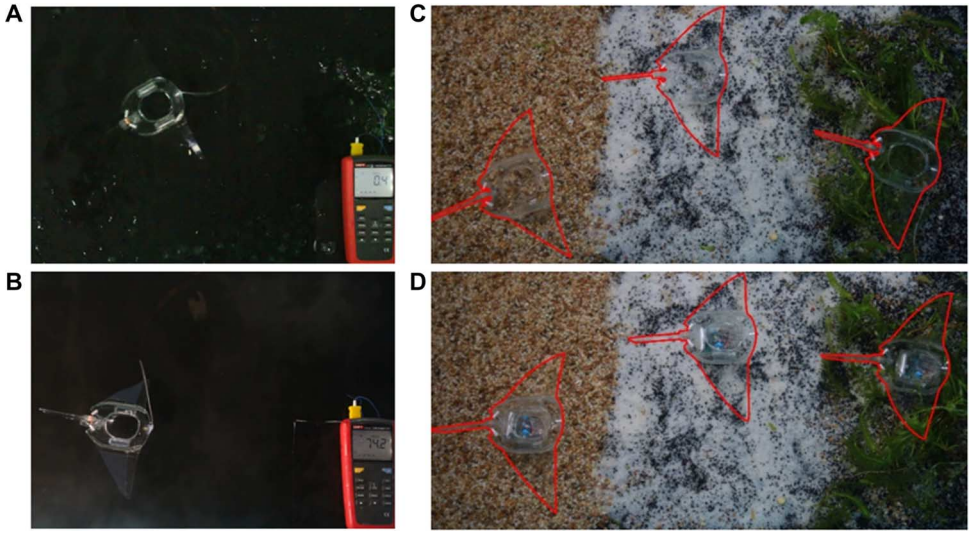

Fig. 6. The thermal tolerance and visual disguise of the fish. The soft robotic fish can swim in a wide range of water temperatures from (**A**) 0.4°C to (**B**) 74.2°C. The stealth sailing of the fish with (**C**) wired power and (**D**) onboard power.

integrating a high-voltage amplifier, a lithium-ion battery, and infrared (IR) remote control circuits (more details can be found in section S6). The system compactness allows the accommodation within the fish. At a first glance, the rigidity of most components in this system is a drawback. To overcome this, the rigid components are sequentially lined up and encapsulated in silicone rubber. The entire package is defined as the electronic pod (Epod), which is glued under the fish body (Fig. 5A). This design does not compromise the necessary softness in the lateral direction. Its added rigidity in the longitudinal direction consequently restrains the undesirable bending in that direction and enhances the robustness of the flapping motions. Despite the additional drag force and relative low power with the Epod, the untethered fish can reach a maximum forward speed of 6.4 cm/s (9.5 kV and 5 Hz), which is roughly half of the tethered version (13.5 cm/s). The speed reduction is mainly caused by a more than doubled increased total weight (from 42.5 to 90.3 g), as well as the additional drag from the Epod (see the Supplementary Materials for detailed discussions). The soft electronic fish can swim and turn under remote control (Fig. 5B). With one single battery charge (3.7 V, 450 mAh), the fish can continuously swim for 3 hours and 15 min at a speed of 1.1 cm/s. In addition, it can make sharp turns under remote IR control while carrying a video camera (Fig. 6D and movie S3). A live video showing the swimming is provided as movie S4, and detailed discussions on the turning performance and the swimming endurance are provided in the Supplementary Materials.

Other notable characteristics of the electronic fish include its excellent environmental adaptability and disguising performance. It can swim well in both cold (0.4°C) and hot (74.2°C) water (Fig. 6, A and B, and movie S5) without any delicate thermal insulation. This is a particular advantage over robots driven by thermally responsive actuators, such as SMAs and temperature-responsive hydrogels (*27*–*29*). In addition, because of the transparency of the major components (movie S6), the fish can blend into various environmental backgrounds, showing high disguising performance (Fig. 6, C and D).

DISCUSSION

In summary, we designed a soft electronic fish with DE as the actuator and encapsulated hydrogel and surrounding water as the highly robust electrodes. Counterintuitively, we showed that the high voltage required for actuating the DE is compatible with the aqueous operating environment. The soft body is designed to function as the transmission that converts the simple in-plane DE actuation into the complex motions necessary for propulsion. Overall, the excellent performance of the DE, when combined with integrated compact electronics for power and remote control, results in exceptional mobility for an untethered electronic fish with a swimming speed of 0.69 body length per second. In addition to the wireless mobility, the electronic fish has other notable attributes, including transparency, long endurance, and temperature tolerance. All these performance features are highly desirable for its operation in harsh environments. Overall, the engineering principle behind our robot design can be potentially useful in guiding device designs for demanding applications such as flexible devices and soft robots.

MATERIALS AND METHODS

Materials

The soft fish body was made of commercial silicone elastomer (SYLGARD 184, heat-cured). The materials used for fabricating hydrogel electrodes are all commercial grades: acrylamide (Sigma-Aldrich), *N*, *N*′-methylenebis (acrylamide) (BIS; Sigma-Aldrich), ammonium persulfate (APS; Sigma-Aldrich), *N*,*N*,*N*′,*N*′-tetramethylethylenediamine (TEMED; Sigma-Aldrich), and lithium chloride (LiCl). For making the hydrogel, acrylamide (2 g) and LiCl (0.1 g) were dissolved in 10 ml of deionized water, and BIS (0.001 g) and APS (0.02 g) were subsequently added into the solution. Next, 20 μl of TEMED was added, and the final solution was poured into a mold and cured for 30 min with ultraviolet light to form the conductive hydrogel membrane. The DE membranes (initial thickness, 1.5 mm) consist of two DE membranes stacked together (3M VHB 4910 and 4905 membranes). Silicone adhesive glue (Dow Corning 734) was used for the sealing and gluing. More details of the fabrication and assembly can be found in figs. S1 to S5.

Performance characterization

When the fish was powered by wired voltage source, a signal generator (Agilent 33220A) and a voltage amplifier (Trek 610E) were combined to

generate the high voltage (Fig. 4A). The three-view videos (Fig. 3, A to C) were recorded by high-definition cameras. The thrust of the fish was measured by a force sensor connected behind the fish and analyzed using a data acquisition software (M400). More details on the thrust measurement are provided in the Supplementary Materials.

Onboard system for power and remote control

A diagram of the compact high oscillating voltage generator is shown in fig. S8. The experimental voltage is 100 times of the simulated voltage signal shown in fig. S8B. The system is powered by a low-voltage battery (3.7 V) with flyback topology to achieve small size, high voltage, and isolation. The system is controlled by an eight-pin microcontroller to tune the voltage frequency and amplitude with IR remote control. The high-voltage amplitude is adjusted by pulse width modulation duty cycle. The oscillating frequency is tuned through an on-off control of an S1 gate driver. The high-voltage circuits consist of the discharge circuits and the rail-to-rail amplifiers, with the latter capable of raising the voltage to a high level and dropping it to zero.

FEA simulation

The results presented in Fig. 2 (C to F) and fig. S9 were calculated using Abaqus 6.13. A material model from a previous study (*25*) was embedded into the software with the user-defined subroutine UMAT. Hybrid, reduced integration elements (C3D8RH) were used in the simulation.

SUPPLEMENTARY MATERIALS

Supplementary material for this article is available at http://advances.sciencemag.org/cgi/content/full/3/4/e1602045/DC1

section S1. Prestretching of DE membranes
section S2. Hydrogel and muscle laminate
section S3. The fin laminate, soft body, and steering tail
section S4. Preliminary attempt to fabricate a soft fish by 3D printing
section S5. Measurements of speed, turning radius, and thrust
section S6. The onboard power and control system (Epod)
section S7. Von Mises stress contours in FEA simulation
section S8. Water conductivity
section S9. Viscous effect of the DE membranes
fig. S1. The prestretch of the DE membrane.
fig. S2. Fabrication of the muscle laminate.
fig. S3. Fabrication of the fin laminate.
fig. S4. Fabrication of the soft body and steering tail.
fig. S5. Buoys and electromagnetic steering tail.
fig. S6. Soft fish by 3D printing.
fig. S7. Von Measurement of the speed and turning radius.
fig. S8. The Epod.
fig. S9. Von Mises stress distribution by FEA.
table S1. Speed and turning radius.
table S2. Capacitance, thrust, power, and efficiency.
table S3. Dimensions and weight of the soft robot fish.
movie S1. The swimming of the tethered powered fish.
movie S2. The flapping and undulatory motions of the fins of an anchored wired fish at various frequencies (1, 3, and 4 Hz).
movie S3. The swimming and turning of an untethered fish with and without a payload (a video camera).
movie S4. Video record captured by an onboard camera on a swimming fish.
movie S5. The swimming of a transparent tethered fish in cold (0.4°C) and hot (74.2°C) water.
movie S6. The swimming of a transparent tethered fish and partially 3D-printed fish.

REFERENCES AND NOTES

1. D. Rus, M. T. Tolley, Design, fabrication and control of soft robots. *Nature* **521**, 467–475 (2015).
2. J. A. Rogers, T. Someya, Y. Huang, Materials and mechanics for stretchable electronics. *Science* **327**, 1603–1607 (2010).
3. D. Trivedi, C. D. Rahn, W. M. Kier, I. D. Walker, Soft robotics: Biological inspiration, state of the art, and future research. *Appl. Bionics Biomech.* **5**, 99–117 (2008).
4. S. Kim, C. Laschi, B. Trimmer, Soft robotics: A bioinspired evolution in robotics. *Trends Biotechnol.* **31**, 287–294 (2013).
5. Y. Mengüç, Y.-L. Park, H. Pei, D. Vogt, P. M. Aubin, E. Winchell, L. Fluke, L. Stirling, R. J. Wood, C. J. Walsh, Wearable soft sensing suit for human gait measurement. *Int. J. Rob. Res.* **33**, 1748–1764 (2014).
6. P. Polygerinos, Z. Wang, K. C. Galloway, R. J. Wood, C. J. Walsh, Soft robotic glove for combined assistance and at-home rehabilitation. *Rob. Auton. Syst.* **73**, 135–143 (2015).
7. M. T. Tolley, R. F. Shepherd, B. Mosadegh, K. C. Galloway, M. Wehner, M. Karpelson, R. J. Wood, G. M. Whitesides, A resilient, untethered soft robot. *Soft Robot.* **1**, 213–223 (2014).
8. R. F. Shepherd, F. Ilievski, W. Choi, S. A. Morin, A. A. Stokes, A. D. Mazzeo, X. Chen, M. Wang, G. M. Whitesides, Multigait soft robot. *Proc. Natl. Acad. Sci. U.S.A.* **108**, 20400–20403 (2011).
9. S. A. Morin, R. F. Shepherd, S. W. Kwok, A. A. Stokes, A. Nemiroski, G. M. Whitesides, Camouflage and display for soft machines. *Science* **337**, 828–832 (2012).
10. S. Seok, C. D. Onal, K.-J. Cho, R. J. Wood, D. Rus, S. Kim, Meshworm: A peristaltic soft robot with antagonistic nickel titanium coil actuators. *IEEE ASME Trans. Mechatron.* **18**, 1485–1497 (2013).
11. M. A. Graule, P. Chirarattananon, S. B. Fuller, N. T. Jafferis, K. Y. Ma, M. Spenko, R. Kornbluh, R. J. Wood, Perching and takeoff of a robotic insect on overhangs using switchable electrostatic adhesion. *Science* **352**, 978–982 (2016).
12. Y.-L. Park, B.-r. Chen, N. O. Pérez-Arancibia, D. Young, L. Stirling, R. J. Wood, E. C. Goldfield, R. Nagpal, Design and control of a bio-inspired soft wearable robotic device for ankle–foot rehabilitation. *Bioinspir. Biomim.* **9**, 016007 (2014).
13. F. Ilievski, A. D. Mazzeo, R. F. Shepherd, X. Chen, G. M. Whitesides, Soft robotics for chemists. *Angew. Chem.* **123**, 1890–1895 (2011).
14. S.-J. Park, M. Gazzola, K. S. Park, S. Park, V. Di Santo, E. L. Blevins, J. U. Lind, P. H. Campbell, S. Dauth, A. K. Capulli, F. S. Pasqualini, S. Ahn, A. Cho, H. Yuan, B. M. Maoz, R. Vijaykumar, J.-W. Choi, K. Deisseroth, G. V. Lauder, L. Mahadevan, K. K. Parker, Phototactic guidance of a tissue-engineered soft-robotic ray. *Science* **353**, 158–162 (2016).
15. J. C. Nawroth, H. Lee, A. W. Feinberg, C. M. Ripplinger, M. L. McCain, A. Grosberg, J. O. Dabiri, K. K. Parker, A tissue-engineered jellyfish with biomimetic propulsion. *Nat. Biotechnol.* **30**, 792–797 (2012).
16. J.-S. Koh, E. Yang, G.-P. Jung, S.-P. Jung, J. H. Son, S.-I. Lee, P. G. Jablonski, R. J. Wood, H.-Y. Kim, K.-J. Cho, Jumping on water: Surface tension–dominated jumping of water striders and robotic insects. *Science* **349**, 517–521 (2015).
17. H.-T. Lin, G. G. Leisk, B. Trimmer, GoQBot: A caterpillar-inspired soft-bodied rolling robot. *Bioinspir. Biomim.* **6**, 026007 (2011).
18. A. D. Marchese, C. D. Onal, D. Rus, Autonomous soft robotic fish capable of escape maneuvers using fluidic elastomer actuators. *Soft Robot.* **1**, 75–87 (2014).
19. C. Laschi, M. Cianchetti, B. Mazzolai, L. Margheri, M. Follador, P. Dario, Soft robot arm inspired by the octopus. *Adv. Robot.* **26**, 709–727 (2012).
20. M. Wehner, R. L. Truby, D. J. Fitzgerald, B. Mosadegh, G. M. Whitesides, J. A. Lewis, R. J. Wood, An integrated design and fabrication strategy for entirely soft, autonomous robots. *Nature* **536**, 451–455 (2016).
21. M. Yamakita, N. Kamamichi, T. Kozuki, K. Asaka, Z.-W. Luo, A snake-like swimming robot using IPMC actuator and verification of doping effect, *IEEE/RSJ International Conference on Intelligent Robots and Systems, 2005*, Edmonton, Alberta, Canada, 2 to 6 August 2005 (IEEE, 2005).
22. A. Firouzeh, M. Ozmaeian, A. Alasty, An IPMC-made deformable-ring-like robot. *Smart Mater. Struct.* **21**, 065011 (2012).
23. F. Carpi, S. Bauer, D. De Rossi, Stretching dielectric elastomer performance. *Science* **330**, 1759–1761 (2010).
24. I. A. Anderson, T. A. Gisby, T. G. McKay, B. M. O'Brien, E. P. Calius, Multi-functional dielectric elastomer artificial muscles for soft and smart machines. *J. Appl. Phys.* **112**, 041101 (2012).
25. X. Zhao, Z. Suo, Method to analyze programmable deformation of dielectric elastomer layers. *Appl. Phys. Lett.* **93**, 251902 (2008).
26. L. Hines, K. Petersen, M. Sitti, Inflated soft actuators with reversible stable deformations. *Adv. Mater.* **28**, 3690–3696 (2016).
27. J. Kim, J. A. Hanna, M. Byun, C. D. Santangelo, R. C. Hayward, Designing responsive buckled surfaces by halftone gel lithography. *Science* **335**, 1201–1205 (2012).
28. L. Ionov, Hydrogel-based actuators: Possibilities and limitations. *Mater. Today* **17**, 494–503 (2014).
29. A. Villanueva, C. Smith, S. Priya, A biomimetic robotic jellyfish (Robojelly) actuated by shape memory alloy composite actuators. *Bioinspir. Biomim.* **6**, 036004 (2011).
30. Z. Su, J. Yu, M. Tan, J. Zhang, Implementing flexible and fast turning maneuvers of a multijoint robotic fish. *IEEE ASME Trans. Mechatron.* **19**, 329–338 (2014).
31. V. Kopman, M. Porfiri, Design, modeling, and characterization of a miniature robotic fish for research and education in biomimetics and bioinspiration. *IEEE ASME Trans. Mechatron.* **18**, 471–483 (2013).

32. H.-J. Kim, S.-H. Song, S.-H. Ahn, A turtle-like swimming robot using a smart soft composite (SSC) structure. *Smart Mater. Struct.* **22**, 014007 (2012).
33. P. Xiao, N. Yi, T. Zhang, Y. Huang, H. Chang, Y. Yang, Y. Zhou, Y. Chen, Construction of a fish-like robot based on high performance graphene/PVDF bimorph actuation materials. *Adv. Sci.* **3**, 1500438 (2016).
34. Z. Wang, G. Hang, J. Li, Y. Wang, K. Xiao, A micro-robot fish with embedded SMA wire actuated flexible biomimetic fin. *Sens. Actuators A Phys.* **144**, 354–360 (2008).
35. Z. Chen, S. Shatara, X. Tan, Modeling of biomimetic robotic fish propelled by an ionic polymer–metal composite caudal fin. *IEEE ASME Trans. Mechatron.* **15**, 448–459 (2010).
36. F. Gao, Z. Wang, Y. Wang, Y. Wang, J. Li, A prototype of a biomimetic mantle jet propeller inspired by cuttlefish actuated by SMA wires and a theoretical model for its jet thrust. *J. Bionic Eng.* **11**, 412–422 (2014).
37. J. J. Hubbard, M. Fleming, V. Palmre, D. Pugal, K. J. Kim, K. K. Leang, Monolithic IPMC fins for propulsion and maneuvering in bioinspired underwater robotics. *IEEE J. Ocean. Eng.* **39**, 540–551 (2014).
38. B. Kim, D.-H. Kim, J. Jung, J.-O. Park, A biomimetic undulatory tadpole robot using ionic polymer–metal composite actuators. *Smart Mater. Struct.* **14**, 1579–1585 (2005).
39. M. Aureli, V. Kopman, M. Porfiri, Free-locomotion of underwater vehicles actuated by ionic polymer metal composites. *IEEE ASME Trans. Mechatron.* **15**, 603–614 (2010).
40. G. Shuxiang, T. Fukuda, K. Asaka, A new type of fish-like underwater microrobot. *IEEE ASME Trans. Mechatron.* **8**, 136–141 (2003).
41. N. Kamamichi, M. Yamakita, K. Asaka, Z. W. Luo, A snake-like swimming robot using IPMC actuator/sensor, *Proceedings 2006 IEEE International Conference on Robotics and Automation*, Orlando, FL, 15 to 19 May 2006 (IEEE, 2006).
42. K. Takagi, M. Yamamura, Z. W. Luo, M. Onishi, S. Hirano, K. Asaka, Y. Hayakawa, Development of a rajiform swimming robot using ionic polymer artificial muscles, *2006 IEEE/RSJ International Conference on Intelligent Robots and Systems*, Beijing, China, 9 to 15 October 2006 (IEEE, 2006).
43. X. Ye, Y. Su, S. Guo, L. Wang, Design and realization of a remote control centimeter scale robotic fish, *IEEE/ASME International Conference on Advanced Intelligent Mechatronics*, Xi'an, China, 2 to 5 July 2008 (IEEE, 2008).
44. X. Tan, D. Kim, N. Usher, D. Laboy, J. Jackson, A. Kapetanovic, J. Rapai, B. Sabadus, X. Zhou, An autonomous robotic fish for mobile sensing, *Proceedings of the 2006 IEEE/RSJ International Conference on Intelligent Robots and Systems*, Beijing, China, 9 to 15 October 2006 (IEEE, 2006).
45. I. A. Anderson, M. Kelch, S. Sun, C. Jowers, D. Xu, M. M. Murray, Artificial muscle actuators for a robotic fish, *Living Machines 2013 Proceedings of the Second International Conference on Biomimetic and Biohybrid Systems*, London, U.K., 29 July to 2 August 2013 (Springer-Verlag, 2013).
46. T. Li, C. Keplinger, R. Baumgartner, S. Bauer, W. Yang, Z. Suo, Giant voltage-induced deformation in dielectric elastomers near the verge of snap-through instability. *J. Mech. Phys. Solids* **61**, 611–628 (2013).
47. J. Shintake, S. Rosset, B. Schubert, D. Floreano, H. Shea, Versatile soft grippers with intrinsic electroadhesion based on multifunctional polymer actuators. *Adv. Mater.* **28**, 231–238 (2016).
48. F. Carpi, D. De Rossi, R. Kornbluh, R. Pelrine, P. Sommer-Larsen, *Dielectric Elastomers as Electromechanical Transducers: Fundamentals, Materials, Devices, Models and Applications of an Emerging Electroactive Polymer Technology* (Elsevier Science, ed. 1, 2008).
49. J. Zhao, J. Niu, D. McCoul, Y. Ge, Q. Pei, L. Liu, J. Leng, Improvement on output torque of dielectric elastomer minimum energy structures. *Appl. Phys. Lett.* **107**, 063505 (2015).
50. C. Keplinger, J.-Y. Sun, C. C. Foo, P. Rothemund, G. M. Whitesides, Z. Suo, Stretchable, transparent, ionic conductors. *Science* **341**, 984–987 (2013).
51. W.-S. Chu, K.-T. Lee, S.-H. Song, M.-W. Han, J.-Y. Lee, H.-S. Kim, M.-S. Kim, Y.-J. Park, K.-J. Cho, S.-H. Ahn, Review of biomimetic underwater robots using smart actuators. *Int. J. Precis. Eng. Manuf.* **13**, 1281–1292 (2012).
52. D. J. Ellerby, How efficient is a fish? *J. Exp. Biol.* **213**, 3765–3767 (2010).

Acknowledgments

Funding: This work was supported by the following programs: National Natural Science Foundation of China (nos. 11572280, 11302190, 11321202, 11432012, U1613202, 21636008, and 11532011), China Association for Science and Technology (Young Elite Scientist Sponsorship Program), and the Chinese central government's Recruitment Program of Global Experts. **Author contributions:** T.L., Z.H., T.X., and W.Y. conceived the concept and wrote the manuscript. G.L., Y.L., T.C., J.D., X.Y., B.L., and Z.Z. carried out the experiments. T.L. and G.L. conducted the mechanical analysis. Y.L. and T.X. guided the material fabrication. T.L., Z.H., T.X., Y.L., and W.Y. directed the project. All authors analyzed and interpreted the data. **Competing interests:** T.L. is applying for a patent related to the described work (CN 205059975 U, 3/2/2016). W.Y. is the director of the Academic Board of the Key Laboratory of Soft Machines and Smart Devices of Zhejiang Province, is a professor at the Department of Engineering Mechanics, Zhejiang University (Hangzhou, China), and is the president of the National Natural Science Foundation of China. The other authors declare that they have no competing interests. **Data and materials availability:** All data needed to evaluate the conclusions in the paper are present in the paper and/or the Supplementary Materials. Additional data related to this paper may be requested from the authors.

Submitted 27 August 2016
Accepted 11 February 2017
Published 5 April 2017
10.1126/sciadv.1602045

Citation: T. Li, G. Li, Y. Liang, T. Cheng, J. Dai, X. Yang, B. Liu, Z. Zeng, Z. Huang, Y. Luo, T. Xie, W. Yang, Fast-moving soft electronic fish. *Sci. Adv.* **3**, e1602045 (2017).